Cytotoxic Effect of Selenium Nanoparticles on Breast Cancer Cell Lines MCF-7 and AMJ13

Hassan Naser Ali[1], Mohanad Waheeb Mahdi[1], Asmaa M. Salih Almohaidi[2] and Kumarss Amini[3]
[1]*Department of Biology, College of Education for Pure Sciences, University of Diyala, 32001 Baqubah, Iraq*
[2]*Biomedical Application Branch, Institute of Laser for Postgraduate Studies, University of Baghdad, 10071 Baghdad, Iraq*
[3]*Department of Microbiology, Islamic Azad University, Saveh Branch, 39514 Saveh, Iran*
{pbio.hassan.naserali, mohanad}@uodiyala.edu.iq, asmaams_bio@csw.uobaghdad.edu.iq, Kumarss@iau.ac.ir

Keywords: Breast Cancer, Selenium Nanoparticles, IC50, MTT Cell Lines, AMJ-13, MCF-7.

Abstract: Selenium nanoparticles, a naturally occurring substance, have a significant impact on modern medical treatment. The synthesis of Se NPs utilizing Na2Seo3 salt as precursor materials is reported in this study. The characteristics of the nanoparticles were FTIR and XRD. The FTIR spectrum showed several numbers of a peak at the wavenumber of 3454.51 cm -1 and 1544. 98 cm^{-1} for O-H stretching, 2902. 87 cm^{-1} It indicates the vibration of the bonds in the methylene or methyl groups (CH2/CH3), confirming the organic nature of the materials surrounding the nanoselenium, 1635. 64 cm^{-1} This deep, sharp peak is crucial, It denotes the existence of an amide bond in proteins or a carbonyl group in organic acids, the XRD peaks at 2θ=17.86 [426.89], 21.68[764.15], 27.63[668.59], 36.51[298.07] from this data can average particle size of Se NPs was calculated to be 5.135 nm. Finding the dose-dependent impact of selenium on the growth of the MCF-7, AMJ13, and NHF cell lines was the aim of the current study. The cytotoxicity of the selenium nanoparticles was examined using breast cancer cell lines. The Methyl thiazolyltetrazolium (MTT) assay was used to determine the median inhibitory concentration (IC50). The IC50 values for selenium were 18.52 µg/mL for AMJ-13, 6.382 µg/mL for MCF-7, and 273.1 µg/mL for the normal NHF cell line.First. At varying concentrations, selenium hindered the cells' ability to proliferate of 100, 50, 25, 12.5, 6.2, 3.1 ug/mL for AMJ-13 (63.35%, 40.11%, 31.3%, 27.2%, 17.41%, and 13.91%). Respectively and for MCF-7 at the same concentration (70.75, 64.41, 50.56, 47.14, 37.7 and 27.68). To sum up, Selenium NPs displays strong cytotoxicity against the AMJ13 and MCF-7 breast cancer cell lines. It is possible to draw the conclusion that selenium has a dose-dependent impact on the growth of MCF-7, AMJ13, and NHF. Furthermore, apoptosis and morphological alterations greatly intensify the growth inhibition.

1 INTRODUCTION

Due to the potential importance of selenium nanoparticles, or SeNPs, for a wide range of physiological functions, research on these particles has become increasingly relevant in recent years. When combined with regular dosage, selenium nanoparticles yield higher absorption than selenium [1]. New methods are needed to make selenium molecules (selenoproteins, selenoenzymes, and the like) more transportable, bioavailable, and bioactive [2]. In addition to being manufactured for nutritional fortification and developed for medicinal uses, SeNPs is in a highly stable colloidal state and has shown several biological functions, including immune system, anti-oxidation, anti-virus, and anti-cancer properties [3]. With its antioxidant, antibacterial and anticancer selenium nanoparticles show great promise for use in novel biomedical and pharmaceutical applications [4].

Breast cancer ranks second in terms of cancer-related mortality and is the most prevalent invasive malignancy in women. Surgery is frequently followed by chemotherapy, immunotherapy, radiation therapy, or a combination of these treatments when breast cancer reaches an advanced stage. Research by Eltouny (2025) indicates that metastatic breast cancer is the most dangerous and incurable form of the disease [5]. Research using breast cancer cells in vitro showed that selenium treatment reduced the growth of the malignant cells, because selenium has anticancer properties and might lessen the side effects of chemotherapy, such as lymphedema, taking selenium supplements may be beneficial for those

with advanced breast cancer [6], [7]. Although selenium has been used for many purposes, such as as a medication to cure cancer, its effects on microorganisms have not yet been well studied. In this study, we examined the impact of selenium nanoparticles (SeNPs) on the AMJ-13 and MCF-7 breast cancer cell lines.

2 MATERIALS AND METHODS

2.1 Selenium Preparation

Preparation of selenium nanoparticles. The production of selenium nanoparticles began with utilising 1 mM plant extract; 0.0189 g of sodium selenate (Na_2SeO_3) is dissolved in 100 ml of deionised water to achieve a 1 mM solution. The plant extract is formulated by dissolving 10 g of green tea plant in 100 ml of deionised water, followed by heating the mixture to 60°C for 10 minutes with a magnetic stirrer to facilitate the extraction of active compounds. The solution is subsequently filtered with filter paper to get pure plant extract. The obtained Na_2SeO_3 is positioned on a magnetic stirrer and heated to 80°C, after which the extract plant solution is gradually introduced to the sodium selenate salts while maintaining continuous stirring. The temperature of the combination was incrementally increased, ensuring it did not surpass 100°C, and agitated for 60 minutes until the solution became dark orange as shown in Figure 1 signifying the synthesis of SeO_2 nanoparticles The research that was done [8].

2.2 Characterization to SeNps

The functional groups that were presented on the surface of the selenium nanoparticles which were synthesized employing the *Camellia sinensis* extract were identified using the FTIR (Fourier Transform Infrared) spectrum analysis, while X-ray diffraction (XRD) analysis was conducted to study the crystalline nature of the synthesized selenium nanoparticles as they showed diffraction peaks values that each corresponds to Braggs equation peaks.

2.3 Cell Culture Preparation

The Iraqi Center for Cancer and Medical Genetic Research Cell Bank provided the two cancer cell lines, which were designated for comparison with the normal cell line (NHF) use in our research. The cancer cell lines were recognized as breast cancer (MCF7) and breast cancer (AMJ13). In DMEM supplemented with 10% fetal bovine serum, 100 units/mL penicillin, and 100 µg/mL streptomycin, MCF-7 and NHF cells were cultivated. After that, the cells were passage through Trypsin-EDTA, reseeded twice a week at 80% confluence, and nurtured at 37 °C [9].

After the incubation, the culture media was removed and exposed to a range of concentrations (100, 50, 25, 12.5, 6.2, 3.1 ug/mL) of the prepared selenium nanoparticle were added to the wells. Untreated cells cultured in complete medium alone served as the negative control; since the highest DMSO concentration introduced via the SeNPs suspension was below 0.1% (v/v), a level not expected to affect cell viability, a separate solvent-only DMSO control was not included. The plate was incubated for 72h at 37 °C and 5% Carbon dioxide. Applying the MTT stain: Following a 72-hour treatment period, 28 µL of (2mg/mL) MTT was added to each well. The incubation continued for three hours. The media was carefully removed and 100 µL of solubilizing solution (DMSO) was added to each well and incubated for 15 minutes.

The optical density was measured at 492 nm using a microplate reader. Cytotoxicity% was calculated using the following equation. According to Ali et al. (2023), the ratio of cytotoxicity, or the inhibition rate of cell growth, was calculated as follows:

$$Cytotoxicity\ \% = (OD\ Control - OD\ sample)/OD\ Control \times 100\%,$$

where OD control is the mean optical density of the untreated (control) wells, and OD Sample is the mean optical density of the treated wells, each averaged across three replicate wells [10].

2.3 Statistical Analysis

Cell lines Tukey's ANOVA multiple comparisons test with GraphPad Prism 8 [9]. The values were presented as the mean ± SD of triplicate measurements [11].

3 RESULTS

3.1 Characterization to SeNps

3.1.1 FTIR (Fourier Transform Infrared Spectroscopy)

The spectrum showed several numbers of a peak at the wavenumber of 3454.51 cm -1 and 1544. 98 cm^{-1} for O-H stretching, 2902. 87 cm^{-1} It indicates the vibration of the bonds in the methylene or methyl

groups (CH2/CH3), confirming the organic nature of the materials surrounding the nanoselenium, 1635. 64 cm^{-1} as shown in Figure1. This deep, sharp peak is crucial, It denotes the existence of an amide bond in proteins or a carbonyl group in organic acids.

3.1.2 X-ray diffraction (XRD) Analysis

The XRD diffraction pattern of the biosynthesized selenium nanoparticles (SeNPs) is presented in Figure 2. The pattern is characterized by a prominent, broad featureless hump (amorphous halo) centered between 2θ = 15° and 35°, which is the definitive spectral signature of predominantly amorphous selenium (a-Se). This amorphous nature is attributed to the rapid reduction and stabilization process mediated by the phytoconstituents of the green tea extract, which act as capping agents and restrict long-range atomic crystallization. However, minor, low-intensity sharp reflections were observed superimposed on this broad amorphous background at 2θ values of 17.86°, 21.68°, 27.63°, and 36.51°. These faint diffractions indicate a semi-crystalline nature, signifying the initial nucleation of localized crystalline domains (such as hexagonal selenium, t-Se) within the amorphous matrix. Due to the presence of these emergent crystalline reflections, the average crystallite size of the localized domains was estimated using Scherrer's equation Particle size (D) = $K\lambda/\beta \cos\theta$ where λ is the wavelength of X-ray (1.540 × 10−10 m), K is the proportionality coefficient, also referred as shape factor and its value is 0.9, θ is the Bragg angle and β is the full width at half maximum (FWHM) of the crystalline reflections in radians. Based on the evaluation of these localized reflections, the average crystallite size was calculated to be approximately 5.14 nm. This ultra-fine size falls within the lower and most efficient range of nanoparticles (1 to 100 nm), which correlates with the high surface-area-to-volume ratio typically observed in predominantly amorphous biogenic nanostructures.

3.2 Cytotoxicity of SeNPs Towards Breast Cancer Cell Lines

The cytotoxicity findings of the biosynthesized SeNPs against MCF-7, AMJ-13, and NHF cell lines are presented in Figures 3-6. The results demonstrated a dose-dependent cytotoxicity effect, where the growth inhibition percentage increased significantly with higher concentrations of selenium (Fig. 3). Using the MTT assay, the (IC50) values were determined for each cell line and are comprehensively summarized in Table 1. The SeNPs exhibited prominent anticancer selectivity, showing the highest toxicity against MCF-7 cells(IC50=6.382 µg/ml), followed by AMJ-13 cells (IC50=18.52 µg/ml). Notably, the nanoparticles displayed a much higher (IC50) value against normal NHF cells (IC50=273.1µg/ml. indicating low toxicity toward non-cancerous cells.

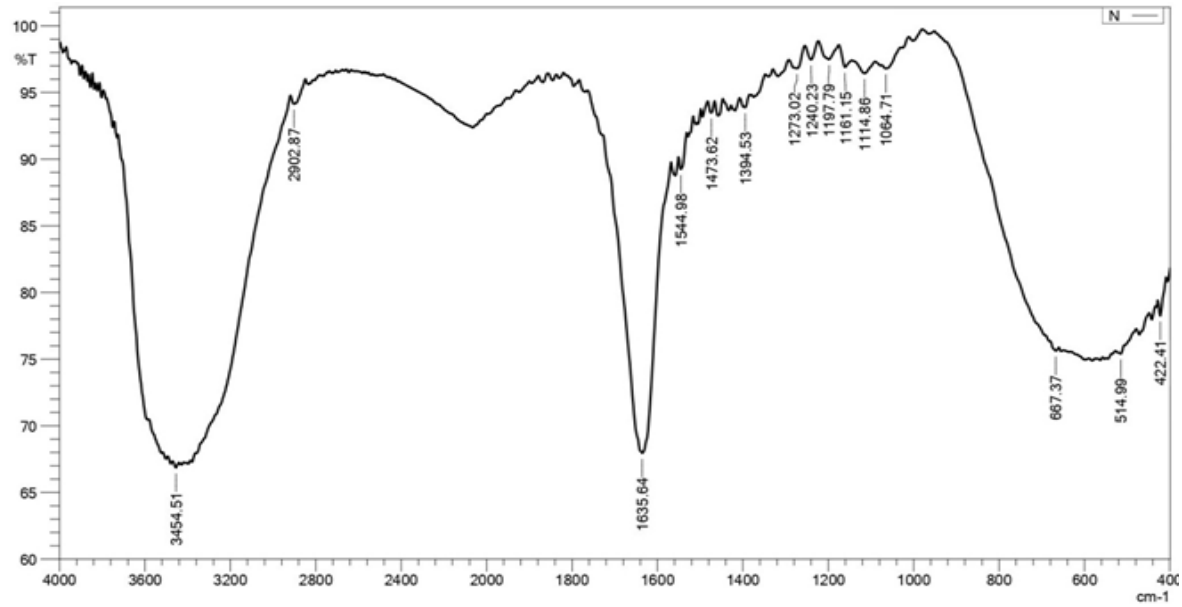

Figure1: FTIR spectra of selenium nanoparticles.

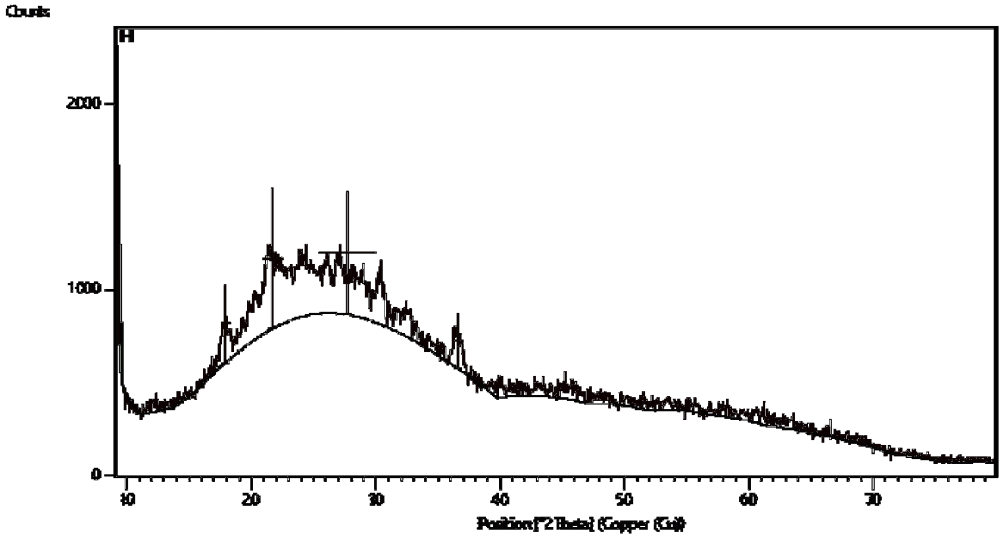

Figure 2: X-ray diffraction pattern of selenium oxide nanoparticles.

Table1: Half-maximal inhibitory concentration (IC50) of the green-synthesized SeNPs against different cell lines.

Cell line	Cell type	IC50Value(µg/ml)
MCF-7	Human Breast Adenocarcinoma	6.382
AMJ-13	Iraqi Breast Cancer	18.52
NHF	Normal Human Fibroblast	273.1

Se NPs' optical density (OD) demonstrated a considerable (ns) effect across all concentrations. In Figure 5, that is explained. SeNPs at used concentrations (100, 50, 25, 12.5, 6.2, and 3.1 ug/mL) transformed into a single cell solution after drug exposure, and the number of cells began to decrease.

As the concentration of Se NPs rises, the number of cells decreases, and the gradual lethal effect grows Figure 6.

4 DISCUSSION

Nanoparticles represent a promising therapeutic frontier with significant future potential, driving substantial local and global research into their biomedical applications [12].

In the current investigation, the cytotoxicity of the biosynthesized selenium nanoparticles (SeNPs) was evaluated in a dose-dependent manner (ranging from 3.1 to 100 ug /mL) against the first continuous breast cancer cell line derived from an Iraqi patient (AMJ-13), alongside MCF-7 and normal NHF cell lines. The MTT assay results demonstrated a classic dose-dependent profile, where increasing SeNPs concentrations significantly enhanced growth inhibition and cytotoxicity.

The quantitative efficacy of this treatment was established through the determination of (IC50) values. Remarkably, the green-synthesized SeNPs exhibited a highly potent and selective antitumor effect, showing the lowest (IC50) against MCF-7 cells (6.382 ug /mL), followed closely by the AMJ-13 cells (18.52 ug/mL). In stark contrast, the (IC50) value against normal NHF cells was found to be exceptionally high (273.1 ug g/mL).

This high therapeutic index underscores a remarkable selectivity, which can be attributed to the synergistic action between the selenium core and the bio-organic capping layer derived from green tea. Green tea extract is rich in epigallocatechin gallate (EGCG), a powerful polyphenol possessing inherent antitumor properties that simultaneously acts as a stabilizing and reducing agent during synthesis [13]. The resulting ultra-fine SeNPs (~5.14 nm) possess an enhanced surface area to volume ratio, facilitating superior intracellular penetration across the compromised membranes of malignant cells to trigger localized cytotoxicity, while remaining biocompatible with healthy tissues [14]. Mechanistically, the pronounced cytotoxicity against MCF-7 and AMJ-13 cell lines can be explained through several interconnected cell death pathways. Chief among these is Oxidative Stress mediated by the ROS pathway. At supra-nutritional dosages, biogenic SeNPs act as pro-oxidants, inducing an excessive accumulation of intracellular free radicals

within the cancer microenvironment. This massive ROS influx disrupts mitochondrial membrane potential, destroying the cellular powerhouses and triggering the intrinsic apoptotic cascade [15], like a "double-edged sword," SeNPs and their constituents can have pro-oxidant or antioxidant properties at supra-nutritional dosages.

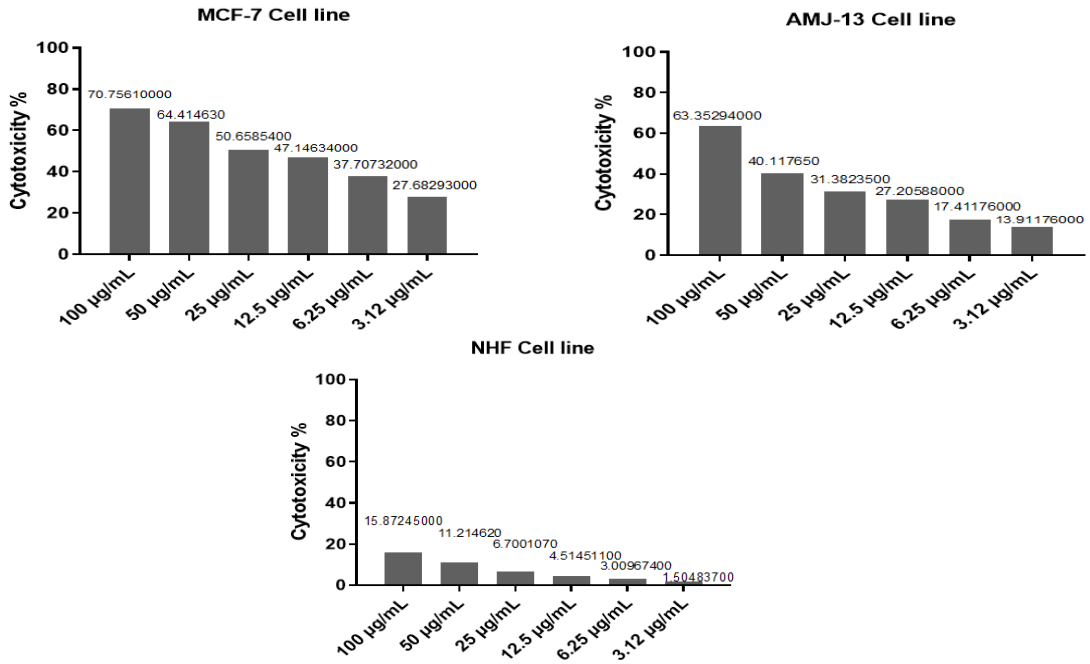

Figure 3: Cytotoxicity effect (CT %) of selenium in different concentration on MCF-7, AMJ-13 and NHF cells.

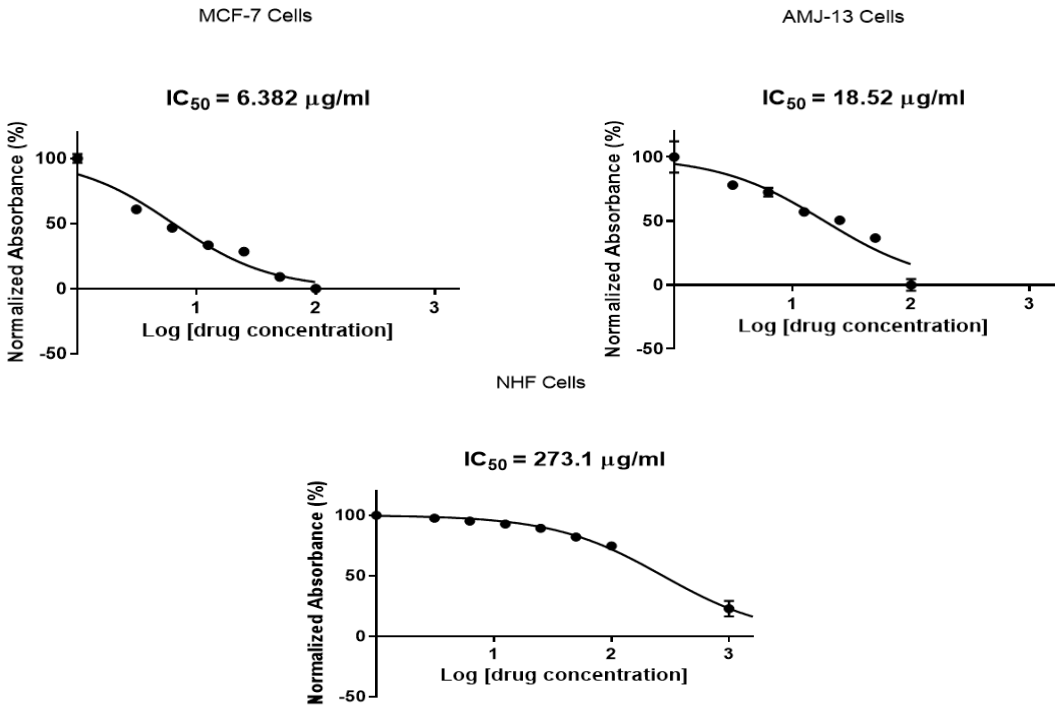

Figure 4: Half maximal inhibitory concentration (IC50) after exposure of the MCF-7, AMJ-13 and NHF cell lines to Se NPs in different concentrations.

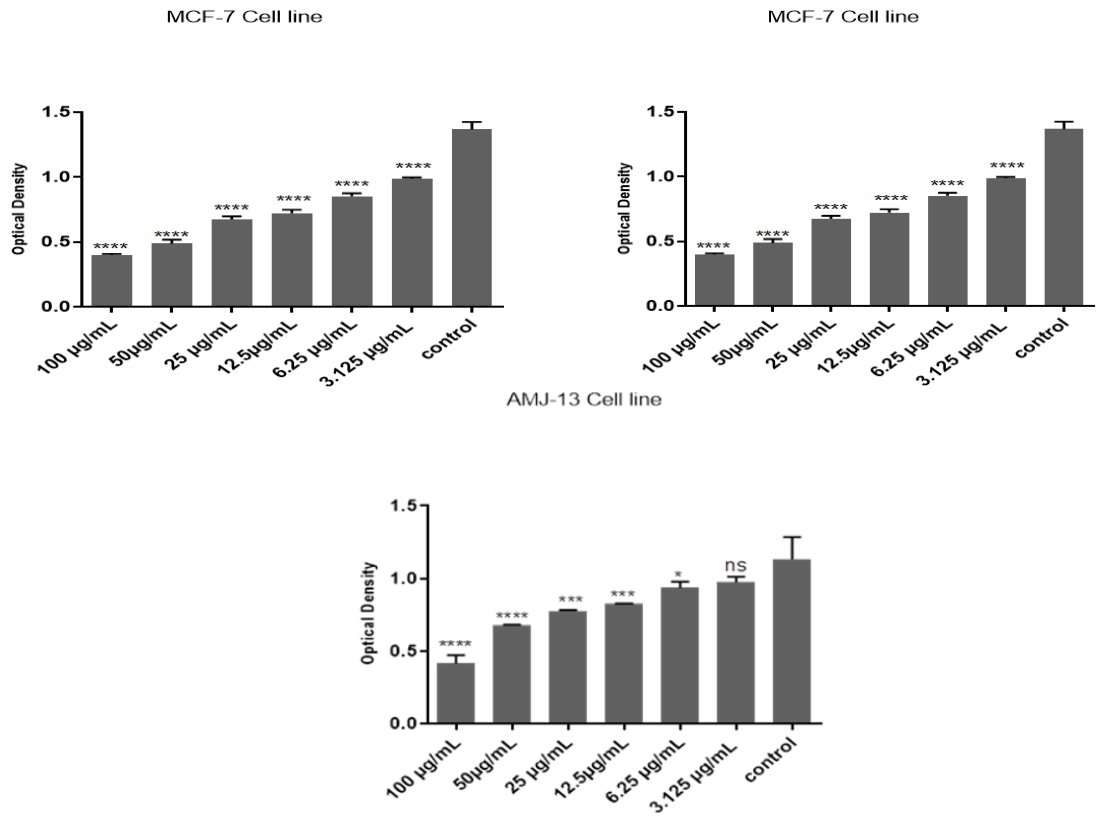

Figure 5: Optical density of Se NPs in different concentrations on MCF-7, AMJ-13 and NHF cell lines.

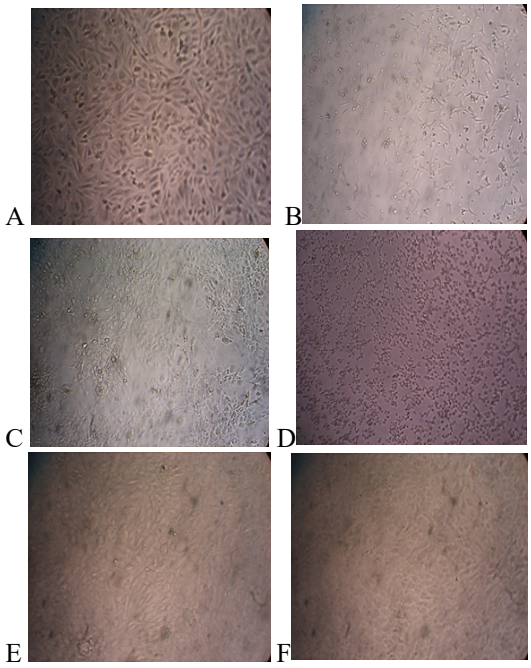

Figure 6: Morphological pictures for MCF-7(A, B), AMJ-13(C, D) and NHF (E, F) cell lines. (before treatment were a full number of cells, and after treatment) monolayer cell shape (An inverted microscope,10x).

Beyond classic apoptosis, the ultra-fine size and surface chemistry of these SeNPs are highly likely to provoke alternative programmed cell death pathways, notably ferroptosis [16]. The internalized SeNPs interact with intracellular glutathione (GSH) reserves. In cancer cells, an overwhelming influx of selenium depletes GSH, which subsequently inactivates glutathione peroxidase 4 (GPX4). The inhibition of this crucial antioxidant enzyme facilitates the unregulated accumulation of lethal lipid peroxides within the cellular membranes, driving iron-dependent, non-apoptotic regulated cell death [17]. This multi-pathway mechanism (combining ROS-driven apoptosis and potential ferroptotic induction) explains the superior susceptibility of the AMJ-13 and MCF-7 breast cancer lines to the synthesized SeNPs, establishing them as highly effective candidates for targeted breast cancer therapy [18].

5 CONCLUSIONS

Selenium nanoparticles (SeNPs) have been shown to be highly effective anticancer agents through biosynthesis. A degree of bio selectivity was

demonstrated by the results, which revealed significant cytotoxic effects when treating the MCF-7 and AMJ-13 cell lines while showing a safe effect on the normal NHF cell line. Additionally, the superiority of the biosynthetic particles in preventing the proliferation of cancer cells was demonstrated by the lower IC50 values (median fatal dosages) in cancer cells when compared to normal cells. The findings also demonstrated that raising the concentration of nanoparticles enhanced the inhibition of cell growth, as demonstrated by morphological alterations and apoptosis, which in turn triggered oxidative stress and raised the generation of ROS.

ACKNOWLEDGMENTS

The authors appreciate the College of Education for Pure Sciences - University of Diyala - for using laboratories with the necessary equipment to carry out the experiment.

REFERENCES

[1] H. N. Ali, A. M. S. Almohaidi, and M. W. M. Alzubadiy, "Effect of green selenium nanosynthesis on Staphylococcus aureus," in Proc. Int. Conf. Applied Innovation in IT, vol. 13, no. 2, pp. 873-879, Jun. 2025.

[2] C. Wen, X. He, J. Zhang, G. Liu, and X. Xu, "A review on selenium-enriched proteins: Preparation, purification, identification, bioavailability, bioactivities and application," Food Funct., vol. 13, no. 10, pp. 5498-5514, 2022.

[3] T. Zhang, M. Qi, Q. Wu, P. Xiang, D. Tang, and Q. Li, "Recent research progress on the synthesis and biological effects of selenium nanoparticles," Front. Nutr., vol. 10, p. 1183487, 2023, [Online]. Available: https://doi.org/10.3389/fnut.2023.1183487.

[4] C. Ferro, H. F. Florindo, and H. A. Santos, "Selenium nanoparticles for biomedical applications: From development and characterization to therapeutics," Adv. Healthcare Mater., vol. 10, no. 16, p. 2100598, 2021.

[5] A. L. E. M. Eltouny, "Cancer: Is it really incurable? A review," EC Cancer, vol. 2, pp. 1-10, 2025.

[6] O. A. Abozaid, L. A. Rashed, S. M. El-Sonbaty, A. I. Abu-Elftouh, and E. S. Ahmed, "Mesenchymal stem cells and selenium nanoparticles synergize with low dose of gamma radiation to suppress mammary gland carcinogenesis via regulation of tumor microenvironment," Biol. Trace Elem. Res., vol. 201, no. 1, pp. 338-352, 2023.

[7] E. G. Varlamova, "Selenium-containing compounds in breast cancer therapy," Biol. Trace Elem. Res., pp. 1-24, 2026.

[8] K. Anu, G. Singaravelu, K. Murugan, and G. Benelli, "Green synthesis of selenium nanoparticles using garlic cloves (Allium sativum): Biophysical characterization and cytotoxicity on Vero cells," J. Cluster Sci., vol. 28, no. 1, pp. 551-563, 2017.

[9] M. I. Salman, A. M. Al-Shammari, and M. A. Emran, "3-Dimensional coculture of breast cancer cell lines with adipose tissue-derived stem cells reveals the efficiency of oncolytic Newcastle disease virus infection via labeling technology," Front. Mol. Biosci., vol. 9, p. 986, 2022.

[10] Y. H. Ali, S. N. Muslim, and I. H. Hamzah, "Assessing the efficacy of dextran and dextransucrase in modulating MCF-7 breast cancer cell activity," Al-Kufa Univ. J. Biol., vol. 15, no. 3, pp. 20-27, 2023.

[11] A. M. Al-Shammari and M. I. Salman, "Antimetastatic and antitumor activities of oncolytic NDV AMHA1 in a 3D culture model of breast cancer," Front. Mol. Biosci., vol. 11, p. 1331369, 2024.

[12] Z. T. Khodair et al., "Synthesis of copper oxide nanoparticles (CuO-NPs) and its evaluation of antibacterial activity against P. aeruginosa biofilm genes," in AIP Conf. Proc., vol. 2190, no. 1, p. 020006, Dec. 2019.

[13] J. W. Oh, M. Muthu, S. S. C. Pushparaj, and J. Gopal, "Anticancer therapeutic effects of green tea catechins (GTCs) when integrated with antioxidant natural components," Molecules, vol. 28, no. 5, p. 2151, 2023.

[14] S. Anjum et al., "Selenium nanoparticles in cancer therapy: Unveiling cytotoxic mechanisms and therapeutic potential," Cancer Rep., vol. 8, no. 6, p. e70210, 2025.

[15] L. V. Belskaya and E. I. Dyachenko, "Oxidative stress in breast cancer: A biochemical map of reactive oxygen species production," Curr. Issues Mol. Biol., vol. 46, no. 5, pp. 4646-4687, 2024.

[16] Z. Chen, H. Lai, L. Hou, and T. Chen, "Rational design and action mechanisms of chemically innovative organoselenium in cancer therapy," Chem. Commun., vol. 56, no. 2, pp. 179-196, 2020.

[17] B. R. Stockwell, X. Jiang, and W. Gu, "Emerging mechanisms and disease relevance of ferroptosis," Trends Cell Biol., vol. 30, no. 6, pp. 478-490, 2020.

[18] B. Wang et al., "ROS-induced lipid peroxidation modulates cell death outcome: Mechanisms behind apoptosis, autophagy, and ferroptosis," Arch. Toxicol., vol. 97, no. 6, pp. 1439-1451, 2023.